

Original Investigation

Correlation of 3-Dimensionally Quantified Intraretinal and Subretinal Fluid With Visual Acuity in Neovascular Age-Related Macular Degeneration

Sebastian M. Waldstein, MD; Ana-Maria Philip, MD; Roland Leitner, PhD; Christian Simader, MD; Georg Langs, PhD; Bianca S. Gerendas, MD; Ursula Schmidt-Erfurth, MD

IMPORTANCE Robust and sensitive imaging biomarkers for visual function are an unmet medical need in the management of neovascular age-related macular degeneration.

OBJECTIVE To determine the correlation of 3-dimensionally quantified intraretinal cystoid fluid (IRC) and subretinal fluid (SRF) with best-corrected visual acuity (BCVA) in treatment-naïve neovascular age-related macular degeneration and during antiangiogenic therapy.

DESIGN, SETTING, AND PARTICIPANTS Retrospective cohort study between November 2009 and November 2011 at an institutional referral center and reading center of patients with treatment-naïve subfoveal choroidal neovascularization receiving intravitreal ranibizumab or aflibercept over 12 months. All individual IRC and SRF lesions were manually delineated on each of the 128 B-scan sections of spectral-domain optical coherence tomographic volume scans at baseline and months 1, 6, and 12. Correlations were computed between the IRC and SRF parameters and the baseline BCVA, final BCVA, and BCVA change. A systematic parameter search was conducted to detect annotation-derived variables with best predictive value. An exponential model for BCVA change balancing for the ceiling effect was constructed.

MAIN OUTCOMES AND MEASURES Goodness of fit of correlations between the IRC and SRF parameters and the baseline BCVA, final BCVA, and BCVA change.

RESULTS Thirty-eight patients were included (25 female, 13 male; mean [SD] age at enrollment, 78.49 [8.23] years; mean [SD] BCVA score at baseline, 54 [16] Early Treatment Diabetic Retinopathy Study letters [Snellen equivalent approximately 20/160], with a gain to 63 [19] letters [Snellen equivalent approximately 20/100] at month 12). A total of 19 456 scans underwent complete quantification of IRC and SRF. The best correlation with BCVA at baseline was achieved using a coverage-based, foveal area-weighted IRC parameter ($R^2 = 0.59$; $P < .001$). The same baseline parameter also predicted BCVA at 12 months ($R^2 = 0.21$; $P = .003$). The BCVA gain correlated with IRC decrease in the exponential model ($R^2 = 0.40$; $P < .001$) and linear model ($R^2 = 0.25$; $P = .002$). No robust associations were found between SRF and baseline BCVA ($R^2 = 0.06$; $P = .14$) or BCVA change ($R^2 = 0.14$; $P = .02$).

CONCLUSIONS AND RELEVANCE In this proof-of-principle study, IRC-derived morphometric variables correlated well with treatment-naïve BCVA and BCVA outcomes in antiangiogenic therapy. While IRC reduction was associated with BCVA gains, some IRC-mediated neurosensory damage remained permanent.

JAMA Ophthalmol. 2016;134(2):182-190. doi:10.1001/jamaophthalmol.2015.4948
Published online December 10, 2015.

 Supplemental content at jamaophthalmology.com

Author Affiliations: Vienna Reading Center, Department of Ophthalmology and Optometry, Christian Doppler Laboratory for Ophthalmic Image Analysis, Medical University of Vienna, Vienna, Austria (Waldstein, Philip, Leitner, Simader, Gerendas, Schmidt-Erfurth); Computational Imaging Research Laboratory, Department of Biomedical Imaging and Image-Guided Therapy, Christian Doppler Laboratory for Ophthalmic Image Analysis, Medical University of Vienna, Vienna, Austria (Langs).

Corresponding Author: Ursula Schmidt-Erfurth, MD, Department of Ophthalmology and Optometry, Medical University of Vienna, Spitalgasse 23, AT-1090 Vienna, Austria (ursula.schmidt-erfurth@meduniwien.ac.at).

Antiangiogenic therapy using intravitreal anti-vascular endothelial growth factor (VEGF) agents is extremely effective at preserving visual function in choroidal neovascularization (CNV) and has become the leading treatment approach in neovascular age-related macular degeneration (nAMD).^{1,2} Similarly, spectral-domain optical coherence tomography (OCT) has become the leading diagnostic tool in the management of AMD.^{3,4} Substantial efforts have been made to combine these 2 advances, using OCT to guide anti-VEGF therapy. However, few published studies have been successful in meeting this goal and the initial excellent reports could not be fully replicated on a large scale.⁵⁻⁹

High-resolution raster scanning by modern OCT delivers a vast amount of morphologic information, but quantification of these data is difficult and has thus far failed to show robust correlation with vision. In particular, central retinal thickness—a variable that is easy to measure—was largely unsuccessful as a surrogate imaging biomarker.¹⁰ However, several large-scale studies demonstrated that the qualitative characterization of CNV-associated fluid (ie, presence or absence of intraretinal cystoid fluid [IRC], subretinal fluid [SRF], and pigment-epithelial detachment) affects individual visual acuity (VA) and response to antiangiogenic treatment.¹¹⁻¹⁴ To further complicate structure-function correlations, the change of VA during treatment is strongly affected by individual baseline VA levels (ie, the ceiling effect).

The identification of quantitative imaging biomarkers that could guide anti-VEGF treatment successfully and allow individualized disease management represents a substantial unmet medical need. Based on the proven effect of CNV-associated fluid on visual function, we hypothesized that a 3-dimensional quantification of such fluid would enable quantitative variables to be correlated with visual function, surpassing the qualitative categorization used previously. In this proof-of-principle study, we manually segmented 2 selected morphologic components, IRC and SRF, in spectral-domain OCT volume scans of a cohort of patients receiving standardized antiangiogenic therapy for nAMD. Variables derived from the segmentation of the lesions were systematically correlated with VA at the treatment-naïve stage. A mathematical model for VA change over time depending on morphologic changes and accounting for the ceiling effect was designed. Finally, predictors for VA outcomes at 1 year were established.

Methods

Patient Population, Treatment, and Imaging

This analysis included data from 38 patients with treatment-naïve active subfoveal CNV secondary to AMD undergoing anti-VEGF therapy at the Department of Ophthalmology and Optometry, Medical University of Vienna in prior prospective studies between November 2009 and November 2011. A retina specialist clinically diagnosed AMD in consideration of results on fundus examination, OCT, and angiography. Detailed inclusion and exclusion criteria are listed in the eAppendix in the [Supplement](#). This retrospective cohort study adhered to the tenets of the Declaration of Helsinki. Ethics ap-

At a Glance

- Three-dimensional segmentation of intraretinal cystoid fluid and subretinal fluid was performed to attempt correlation between fluid-derived variables, baseline visual acuity, and vision outcomes after 12 months of antiangiogenic therapy.
- Intraretinal cystoid fluid correlated well with visual acuity levels at baseline. The horizontal extension of the fluid as well as localization near the foveal center were the most important factors determining the effect on visual acuity.
- The amounts of intraretinal cystoid fluid at baseline were associated with visual acuity outcomes at month 12.
- A reduction in intraretinal cystoid fluid during therapeutic intervention was linearly associated with a gain in vision.
- This study did not find a robust association between subretinal fluid, visual acuity, and treatment outcomes.

proval was obtained from the Ethics Committee at the Medical University of Vienna. All participants provided written informed consent.

After a loading dose consisting of 3 monthly injections, each patient received a fixed regimen of ranibizumab or aflibercept until month 12. Twenty patients received 0.5 mg of ranibizumab monthly, 6 received 0.5 mg of aflibercept monthly, 6 received 2.0 mg of aflibercept monthly, and 6 received 2.0 mg of aflibercept every 2 months.

At each monthly visit, patients underwent spectral-domain OCT using Cirrus HD-OCT (Carl Zeiss Meditec). Volume scans of 512 A-scans by 128 B-scans covering a 6 × 6-mm area were acquired. Best-corrected VA (BCVA) testing using Early Treatment Diabetic Retinopathy Study (ETDRS) charts by certified examiners was performed at each visit. For reporting, ETDRS letter scores were also converted to Snellen equivalents.¹⁵

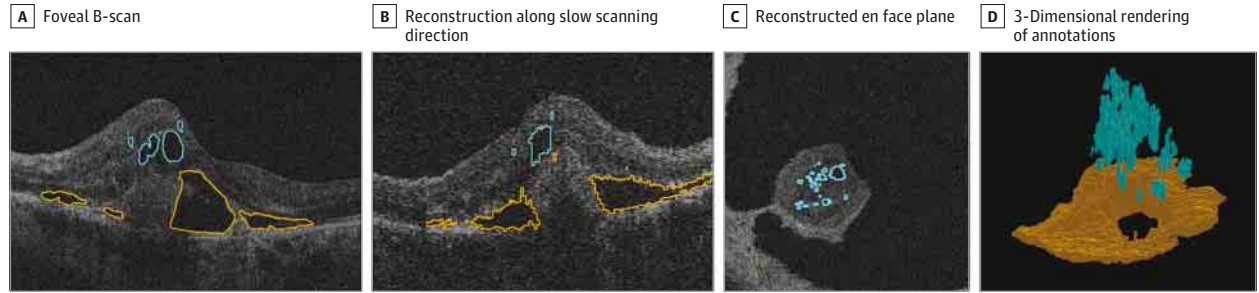
Image Analysis

The visits at baseline (for the treatment-naïve condition) and at months 1, 6, and 12 (for on-treatment effects) were selected for analysis. Spectral-domain OCT imaging data were exported in raw format and evaluated in custom software. Readers trained at the Vienna Reading Center manually delineated IRC and SRF in each of the 128 B-scans contained within each individual OCT volume, and they annotated the position of the foveal center. Detailed information on the annotation procedure, reader training, and reproducibility is provided in the eAppendix in the [Supplement](#). **Figure 1** shows an annotation example. The retrospective image analysis was performed between June 2013 and June 2014.

Structure-Function Correlation

The baseline visit was used to establish correlations between fluid-derived quantitative variables and BCVA at the treatment-naïve condition. As an initial step, to gain understanding of the correlation between fluid lesions and BCVA, linear regression analysis was performed to correlate fluid volume and area in the entire OCT scan and within a cylindrical 3-mm region of interest centered on the fovea with BCVA. Based on the initial

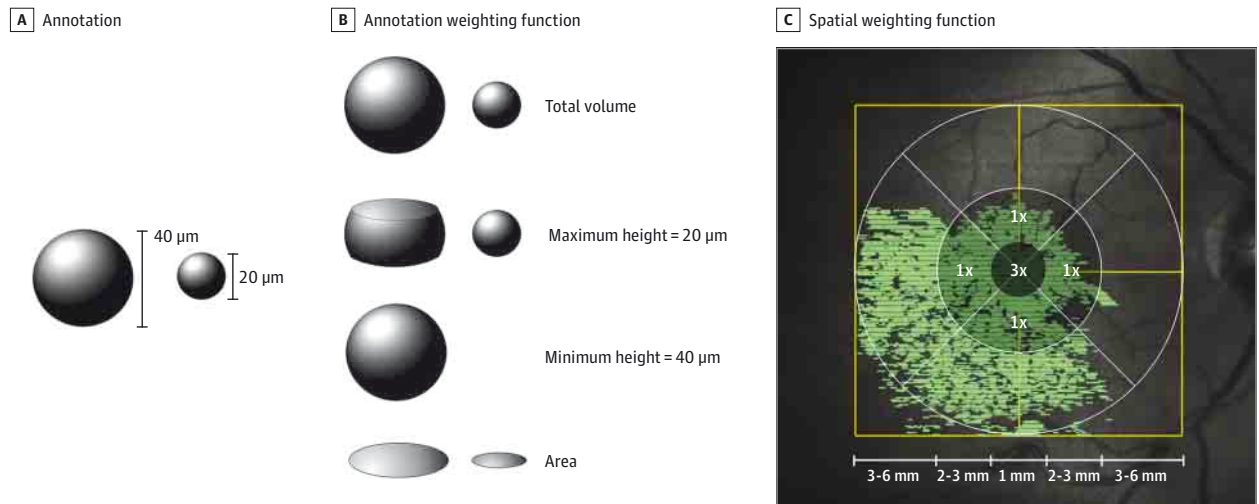
Figure 1. Example of 3-Dimensional Volumetric Annotation of Intraretinal Cystoid Fluid and Subretinal Fluid in Treatment-Naive Neovascular Age-Related Macular Degeneration



Turquoise indicates intraretinal cystoid fluid; orange, subretinal fluid. A, Foveal optical coherence tomographic B-scan (fast scanning direction), where the tracings were performed. B, Reconstruction along the slow scanning direction

(A-scan). C, Reconstructed en face plane (C-scan). D, A 3-dimensional rendering of the annotations.

Figure 2. Illustration of the Annotation Weighting Function $A_{(x,y)}$ and Spatial Weighting Function $S_{(x,y)}$



The annotation weighting function computes various variables out of given fluid annotations. A, Two exemplary spheres with different diameters are shown. B, The annotation weighting function total volume includes the lesions in their entire dimensions, while the maximum and minimum height functions and the area function include only certain aspects of the fluid. C, The spatial weighting

function assigns weights to fluid regions depending on their location in relation to the foveal center. In this case, the central 1-mm area is assigned 3 times the weight of the 2- to 3-mm ring. Fluid regions outside the 3-mm area are not considered. An exemplary en face projection of intraretinal cystoid fluid annotations is shown in green.

results, the availability of complete volumetric representations of the fluid lesions was fully exploited and a broader parameter search was conducted to establish optimal variables for structure-function correlation as follows (Figure 2).

First, the relative effect of the horizontal and/or vertical extension of the fluid regions on BCVA was systematically investigated by introducing various prespecified upper or lower height limits for fluid to be considered in the analysis. To achieve this mathematically, an annotation weighting function $A_{(x,y)}$ was defined, which assigns to each point at the macula (x,y) (ie, each pixel column in the OCT scan) a real number based on the annotated fluid at that said position and the prespecified height limits.

Second, another level of parameter weighting was introduced to account for the physiologic spatial distribution of the cone pho-

toceptors in the macula, with highest packing density (and relevance for BCVA) in the foveola and declining density with increasing eccentricity. To model this effect mathematically, a spatial weighting function $S_{(x,y)}$ was defined to assign differential weights to predefined regions (x,y) on the fundus according to their eccentricity from the foveal center. Further details and the individual step-offs for the weighting procedure are described in the eAppendix in the Supplement.

Finally, a predictor $P_{A,S}$ for correlation with BCVA was computed per individual OCT volume by using the integral $P_{A,S} = \int A \cdot S \, dx \, dy$.

To optimize the analysis of BCVA change over time in consideration of the ceiling effect, an exponential model for BCVA change as a function of morphology change was constructed (eAppendix in the Supplement).

Statistical Analysis

Statistical analysis was performed in a custom-built statistics framework and SPSS version 21 statistical software (IBM Corp). Linear regression analysis was performed to investigate the correlation between fluid-derived variables and baseline BCVA, BCVA at 12 months, and BCVA change from baseline to month 12. The coefficient of correlation (R^2) was computed by ordinary least squares regression and was used as the main outcome measure. Regression lines were fitted using Prism version 6.03 statistical software (GraphPad). All presented mathematical formulae were derived by one of us (R.L.).

Results

Patient Characteristics

All 38 patients had complete examinations at the prespecified visits (baseline and months 1, 6, and 12). Among these patients, 25 were female and 13 were male. The mean (SD) age at enrollment was 78.49 (8.23) years. The mean (SD) BCVA score at baseline was 54 (16) ETDRS letters (Snellen equivalent approximately 20/160), with a gain to 63 (19) letters (Snellen equivalent approximately 20/100) at month 12.

Characteristics of Fluid

In 152 OCT volumes, 7927 fluid regions were manually annotated on 19 456 B-scans. At baseline, 17 eyes showed both IRC and SRF, 8 eyes showed only IRC, and 13 eyes showed only SRF. The mean (SD) horizontal dimension of the individual fluid lesions was 257 (207) μm (range, 12-1785 μm) for IRC and 1354 (1125) μm (range, 12-5977 μm) for SRF. The mean (SD) vertical dimensions were 111 (68) μm (range, 2-590 μm) for IRC and 130 (86) μm (range, 2-528 μm) for SRF. The time required to annotate a typical baseline OCT volume (with the highest average fluid load) was approximately 15 hours. The mean volumes and covered areas for IRC and SRF at the visits evaluated are provided in eTable 1 in the Supplement. All fluid decreased rapidly from baseline to month 1 and then remained minimal.

Correlation of Fluid and Treatment-Naive VA

In the initial analysis using simple variables, correlations were detected for BCVA with IRC volume ($R^2 = 0.40$; $P < .001$) and IRC area ($R^2 = 0.51$; $P < .001$) at baseline. When an OCT subvolume of 3-mm diameter centered on the fovea was selected, the correlations between BCVA and IRC volume ($R^2 = 0.44$; $P < .001$) and between BCVA and IRC area ($R^2 = 0.57$; $P < .001$) improved. Therefore, the retinal area beyond the 3-mm ring was not included in further analysis.

In eTable 2 in the Supplement, we provide the R^2 values of all 135 possible combinations in the comprehensive parameter search using modified predictors $P_{A,S}$ (eAppendix in the Supplement) for the correlation between baseline IRC annotations and baseline BCVA. This parameter search revealed that the best correlation with BCVA could be achieved by a mainly area-based annotation weighting function $A_{x,y}$ (including IRC height only up to a threshold of 20 μm) and a spatial weighting function $S_{(x,y)}$ where the central 1-mm region was assigned a weight of 3 and the remaining 3-mm region was assigned a weight of 1 (eTable

3 in the Supplement). For this particular predictor, the goodness of fit of the linear regression analysis was $R^2 = 0.59$ ($P < .001$). The goodness of fit of the correlations decreased if increasing IRC height components or extrafoveal areas were included in the model (eTable 3 in the Supplement). Figure 3 shows scatterplots for the correlation between the described IRC variables and baseline BCVA.

No robust correlation was found between SRF at baseline and BCVA, either in the entire 6-mm OCT volume using SRF volume ($R^2 = 0.05$; $P = .19$) or SRF area ($R^2 = 0.01$; $P = .64$) or in the central 3-mm subvolume (volume: $R^2 = 0.04$; $P = .23$; area: $R^2 = 0.06$; $P = .14$). No optimization was performed owing to the apparent lack of correlation between SRF and BCVA. Figure 4 shows scatterplots for the correlation between SRF and baseline BCVA.

Multivariate regression analysis was performed to evaluate the combined effect of IRC area and SRF area on baseline BCVA. The multivariate model did not perform better ($R^2 = 0.54$; $P < .001$) than the univariate model just incorporating IRC area. In the model, IRC area remained the only predictor with $P < .05$.

Because the fluid lesions were reduced after a single injection (eTable 1 in the Supplement), no correlations between fluid variables and BCVA were analyzed during the on-treatment phase.

Prediction of VA Outcomes

As the optimized IRC indicator demonstrated the best goodness of fit in correlations with baseline BCVA, this variable was selected for further analyses of BCVA over time. The BCVA at month 12 negatively correlated with the optimized IRC area indicator at baseline ($R^2 = 0.21$; $P = .003$). Using the following exponential model for relative BCVA change in relation to change of the predictor (eAppendix in the Supplement):

$$\ln\left(\frac{BCVA(P_{A,S_2})}{BCVA(P_{A,S_1})}\right) = -\alpha(P_{A,S_2} - P_{A,S_1})$$

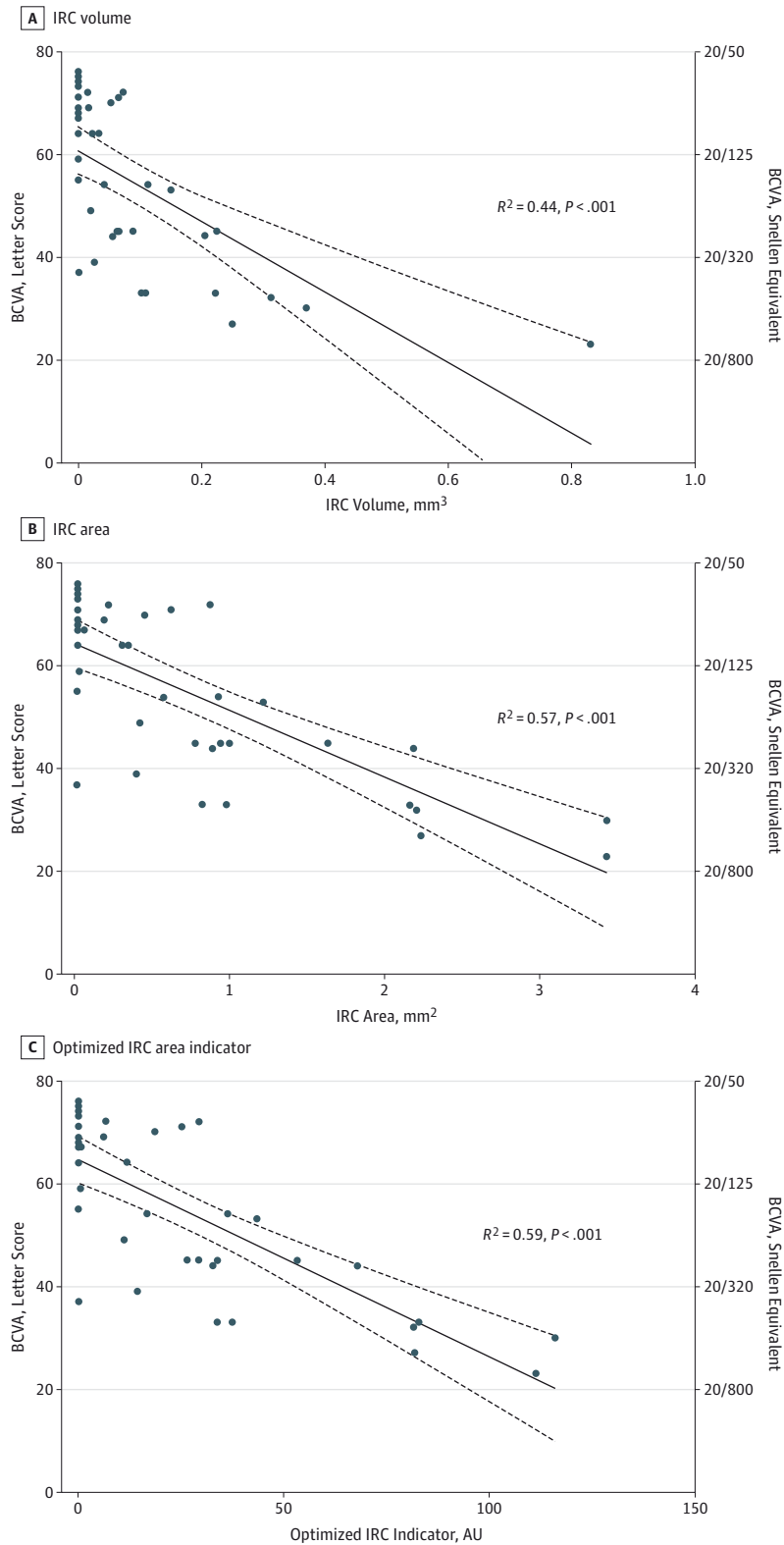
a linear correlation between the relative BCVA change from baseline to month 12 and the change in the optimized IRC parameter was revealed ($R^2 = 0.40$; $P < .001$). This correlation was also present, although weaker, when using absolute BCVA change instead of the exponential model ($R^2 = 0.25$; $P = .002$). Figure 5 shows corresponding scatterplots.

When using SRF area in the exponential BCVA change model, a weak correlation between the change in SRF from baseline to month 12 and relative BCVA change was detected ($R^2 = 0.14$; $P = .02$). Multivariate regression analysis was performed to evaluate the combined effect of IRC and SRF variables on absolute BCVA change ($R^2 = 0.31$; $P = .001$). Again, the IRC-derived area indicator remained the only predictor with $P < .05$.

Discussion

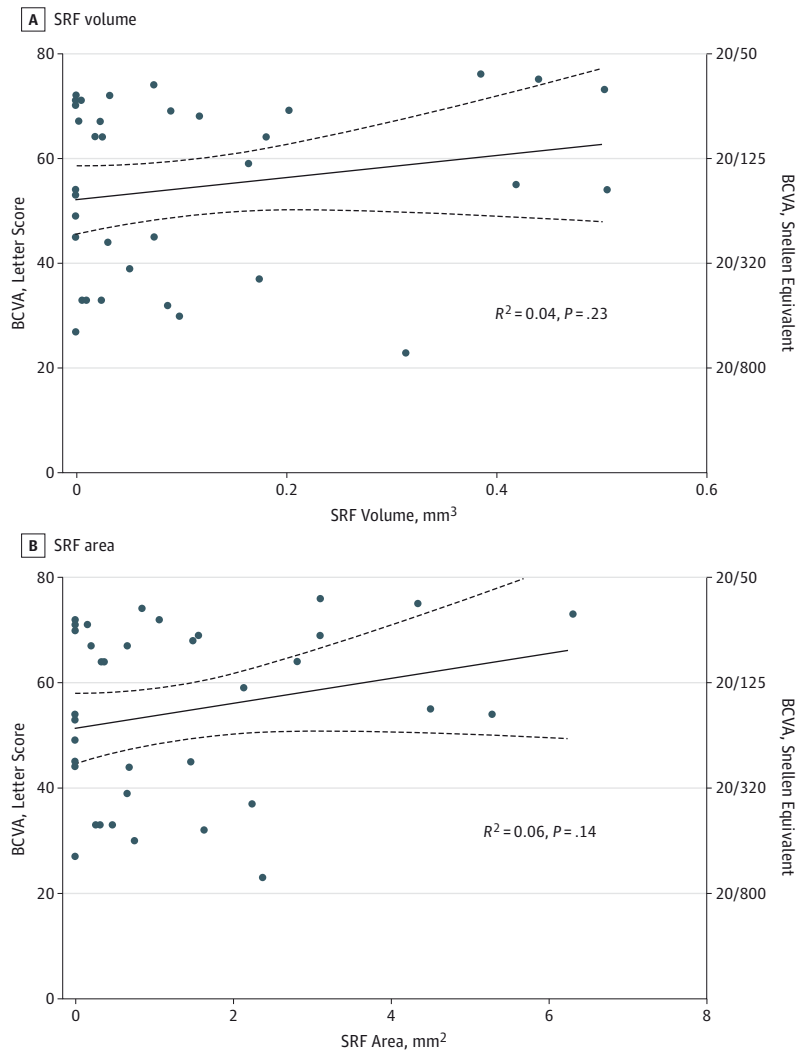
This proof-of-principle study demonstrates that IRC is a quantifiable factor relevant for visual function and treatment response in nAMD. The effect of IRC on BCVA was dependent on the amount (ie, mainly horizontal extension) and location (ie, eccentricity from the fovea). On the other hand, SRF failed to

Figure 3. Correlations Between Intraretinal Cystoid Fluid (IRC)-Derived Variables and Best-Corrected Visual Acuity (BCVA) in Treatment-Naive Neovascular Age-Related Macular Degeneration



Correlations of IRC volume (A), IRC area (B), and optimized IRC area indicator (C) with BCVA. In general, increasing amounts of IRC are associated with worse BCVA. The IRC area (B) shows a better correlation with vision than the IRC volume (A), and the best correlation is achieved with an optimized IRC area indicator accentuating central areas and considering IRC height only up to 20 μ m (C). The clusters of points on the y-axis represent patients without IRC at baseline (34% of the cohort). AU indicates artificial units; solid line, the regression line; and dashed lines, 95% confidence interval of the regression line.

Figure 4. Correlations Between Subretinal Fluid (SRF)-Derived Variables and Best-Corrected Visual Acuity (BCVA) in Treatment-Naive Neovascular Age-Related Macular Degeneration



No robust correlations were detected for SRF volume (A) and area (B) with BCVA. However, eyes with greater amounts of SRF tended to show better BCVA values, indicating a possible protective effect of SRF. Solid line indicates the regression line; dashed lines, 95% confidence interval of the regression line.

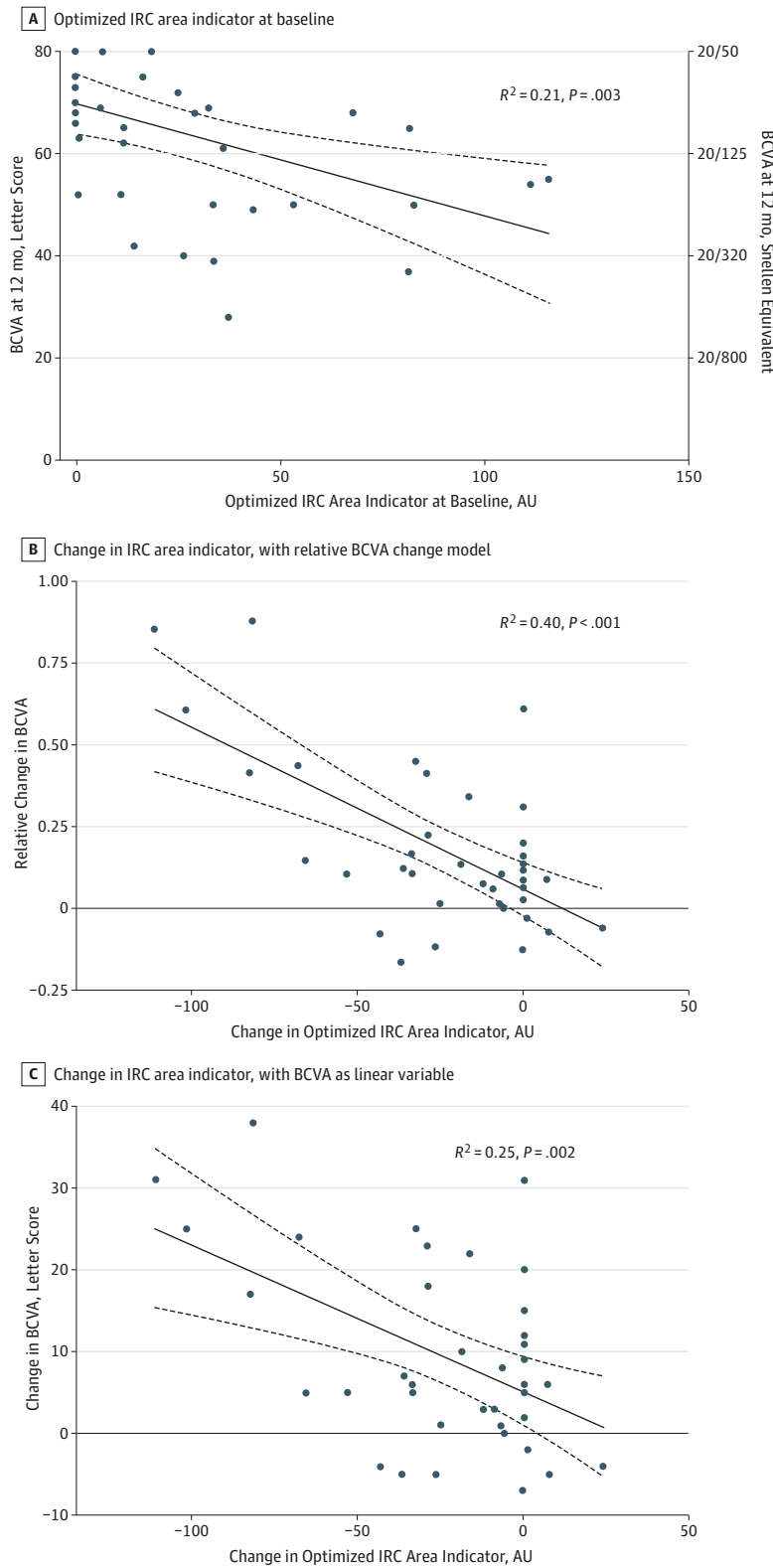
demonstrate robust correlations with BCVA. While we did not consider other potentially important determinants such as photoreceptor integrity, subretinal hyperreflective material, and integrity of the retinal pigment epithelium, our study contributes evidence that high-resolution OCT imaging may provide patient-relevant outcome variables in both practice and research settings.

At the treatment-naive stage, roughly 60% ($R^2 = 0.57$; $P < .001$) of the primary BCVA condition could be predicted by an IRC-derived variable. Importantly, quantification of IRC at baseline could also predict 20% of the final BCVA outcome at 12 months, signifying the irreversible nature of neurosensory damage by intraretinal exudation. When only patients with IRC at baseline and complete resolution of IRC at month 12 were included, this association increased to 30% (eFigure 1 in the Supplement). Finally, 40% of vision change from baseline to month 12 could be explained by the resolution of IRC-related changes over time, using a newly developed mathematical model that accounts for confounding factors such as the ceiling effect.

The fact that IRC is a relevant morphologic element associated with poor VA in nAMD has been reported in several studies. In the Comparison of Age-Related Macular Degeneration Treatments Trials, patients with IRC had on average approximately 2 lines poorer BCVA than patients without IRC,¹¹ which was confirmed in the VIEW (VEGF Trap-Eye: Investigation of Efficacy and Safety in Wet AMD) study.¹⁴ These results were based on dichotomous grading and did not provide a quantitative and spatially resolved analysis. In contrast, our study enables for the first time, to our knowledge, a continuous prediction of BCVA based on volumetric quantification of IRC in consideration of spatial distributions.

A finding of this study was that the IRC-mediated damage to neurosensory function at baseline is only partly reversible by anti-VEGF treatment. Therefore, 20% of 1-year BCVA outcomes could already be predicted at baseline based on quantification of IRC. Eyes with greater amounts of IRC at baseline demonstrated poorer BCVA outcomes at 12 months, irrespective of their

Figure 5. Prediction of Best-Corrected Visual Acuity (BCVA) After 1 Year of Antiangiogenic Therapy



A, Roughly 20% of final BCVA could be predicted by assessment of intraretinal cystoid fluid (IRC) at baseline, signifying that IRC-mediated damage may partially remain permanent. B, Up to 40% of BCVA change from baseline to month 12 could be explained by the resolution of IRC using a relative BCVA change model. C, When using BCVA as a linear variable, the correlation was weaker. AU indicates artificial units; solid line, the regression line; and dashed lines, 95% confidence interval of the regression line.

baseline BCVA levels (eFigure 2 in the Supplement). Our results corroborate previous reports, which were, however, un-

able to quantify this phenomenon.^{11,14} Considering that a certain extent of IRC-related functional damage is irreversible,

future studies in nAMD may require accounting for IRC at baseline for adequate analyses of BCVA change over time.

The clinical implications of our study, while not definitive, are 2-fold. First, our results suggest that IRC at presentation should be treated aggressively until a maximum resolution is achieved, because resolution of IRC seems to translate to functional benefits. Second, patients with extensive IRC at presentation may be counseled that antiangiogenic therapy may likely not lead to full BCVA restoration, as our results suggest an irreversible component of IRC-related neurosensory damage.

This study allows insight into the pathomechanism of functional damage in nAMD. In a systematic parameter search enabled by 3-dimensional annotations, the analysis suggested that area-based variables with an accentuation of central regions correlate best with BCVA. The vertical extension of IRC was relevant only up to a threshold of 20 μm . In other words, how much of the retina was affected by IRC appeared more relevant to visual function than how edematous the individual areas were. Because the vertical component of fluid directly translates into retinal thickness, our findings provide further evidence for the irrelevance of retinal thickness as an imaging biomarker in AMD.¹⁰ Although not directly transferable to our study, Pelosini et al¹⁶ previously demonstrated a correlation between an area-based inverse measure of IRC and BCVA in cystoid macular edema of non-AMD etiology. Accordingly, IRC may cause mechanical damage by stretching the bipolar axons located between the plexiform layers. Our results support this hypothesis, although the pathomechanism leading to vision loss may be more complex in nAMD than in macular edema from other causes. Our approach using full 3-dimensional segmentation of IRC goes beyond the method used by Pelosini and colleagues by accounting for fluid accumulation within all retinal layers, which is impossible using en face-based quantification.¹⁶

It is interesting to note that no robust correlations between SRF and BCVA were found in our study. Recent results from CATT and VIEW demonstrated a beneficial effect of SRF on BCVA, and indeed our experiments show a trend for better BCVA with increasing SRF volume and area.^{11,14} However, our study may have been underpowered to detect such an association. Also in other diseases such as diabetic macular edema or retinal vein occlusion, SRF was associated with improved BCVA outcomes.^{17,18} Whether this apparently protective effect of SRF is directly caused by the fluid or is a consequence of other pathomorphologic processes associated with SRF remains to be clarified.

This study's main limitation is its sample size, which has implications on the generalizability of our results toward the general population. Although the number of patients allowed the detection of robust correlations, the inclusion of larger cohorts may provide better model stability and preci-

sion and may reveal additional effects (such as those caused by SRF). Moreover, the mean baseline VA in our cohort was lower than in typical nAMD trials, which may affect the transferability of our findings toward better-seeing eyes. Indeed, prior studies have demonstrated larger effects of retinal morphology on vision outcomes in individuals with poorer baseline BCVA.¹⁴ Cross-validation of the parameter search using separate training and validation data sets was also not feasible owing to the limited sample size. Given the effort required for manual annotation of IRC in 19 456 individual slices, larger studies will only be feasible using automated fluid quantification methods, which will be available soon.¹⁹

A further limitation of this study is its retrospective nature, which entails disadvantages such as possible lack of data and selection bias. However, because data of prospectively studied cohorts were included, these risks were minimized. As the patient population was specified by predefined criteria (excluding prior treatment, very good and very poor baseline BCVA levels, large hemorrhage, and fibrosis or atrophy), it remains uncertain how our results may apply to the general population of patients with nAMD, in which ocular comorbidities are common. However, based on the inclusion and exclusion criteria, our results may apply well to the typical randomized clinical trial setting.

Furthermore, as only fixed anti-VEGF treatment regimens were used in this study, it is unknown how our results translate to flexible therapeutic regimens. The effects of retinal morphology on treatment outcomes beyond 1 year of follow-up were not studied. Moreover, in addition to IRC and SRF, many other OCT findings in nAMD may show important correlations with visual function, such as the condition of the photoreceptor layer and subretinal neovascular ingrowth or the condition of the retinal pigment epithelium.²⁰⁻²³ Future studies incorporating these structures will add insight into multiple factors positively or negatively affecting BCVA. To optimize extraction of morphological data from spectral-domain OCT, advanced computational image analysis tools are required to clearly visualize and quantify distinct changes.^{24,25}

Conclusions

This study demonstrated that IRC-derived imaging biomarkers have the potential to predict BCVA at the treatment-naïve stage as well as BCVA outcomes in antiangiogenic therapy of nAMD. While the resolution of IRC is associated with BCVA gains, a proportion of IRC-mediated neurosensory damage may remain permanent. If confirmed, our findings may allow improved patient counseling, enable balanced trial designs, and support the development of personalized treatment approaches.

ARTICLE INFORMATION

Submitted for Publication: July 22, 2015; final revision received September 9, 2015; accepted October 16, 2015.

Published Online: December 10, 2015.
doi:10.1001/jamaophthalmol.2015.4948.

Author Contributions: Drs Waldstein and Schmidt-Erfurth had full access to all of the data in

the study and take responsibility for the integrity of the data and the accuracy of the data analysis.

Study concept and design: Waldstein, Leitner, Schmidt-Erfurth.

Acquisition, analysis, or interpretation of data: Waldstein, Philip, Leitner, Simader, Langs, Gerendas.

Drafting of the manuscript: Waldstein.

Critical revision of the manuscript for important intellectual content: Philip, Leitner, Simader, Langs, Gerendas, Schmidt-Erfurth.

Statistical analysis: Waldstein, Leitner, Gerendas.

Obtained funding: Waldstein, Gerendas.

Administrative, technical, or material support: Philip, Simader.

Study supervision: Schmidt-Erfurth.

Conflict of Interest Disclosures: All authors have completed and submitted the ICMJE Form for Disclosure of Potential Conflicts of Interest. Dr Waldstein reported receiving honoraria and nonfinancial support for serving as a consultant to Bayer Healthcare and Novartis. Dr Schmidt-Erfurth reported receiving honoraria and nonfinancial support for serving as a consultant to Alcon, Bayer Healthcare, Boehringer Ingelheim, and Novartis. No other disclosures were reported.

Funding/Support: This study was supported by the Austrian Federal Ministry of Economy, Family and Youth and the National Foundation for Research, Technology and Development and by a grant from the Christian Doppler Research Association.

Role of the Funder/Sponsor: The funders had no role in the design and conduct of the study; collection, management, analysis, and interpretation of the data; preparation, review, or approval of the manuscript; and decision to submit the manuscript for publication.

REFERENCES

- Brown DM, Kaiser PK, Michels M, et al; ANCHOR Study Group. Ranibizumab versus verteporfin for neovascular age-related macular degeneration. *N Engl J Med*. 2006;355(14):1432-1444.
- Rosenfeld PJ, Brown DM, Heier JS, et al; MARINA Study Group. Ranibizumab for neovascular age-related macular degeneration. *N Engl J Med*. 2006;355(14):1419-1431.
- Huang D, Swanson EA, Lin CP, et al. Optical coherence tomography. *Science*. 1991;254(5035):1178-1181.
- Keane PA, Patel PJ, Liakopoulos S, Heussen FM, Sadda SR, Tufail A. Evaluation of age-related macular degeneration with optical coherence tomography. *Surv Ophthalmol*. 2012;57(5):389-414.
- Fung AE, Lalwani GA, Rosenfeld PJ, et al. An optical coherence tomography-guided, variable dosing regimen with intravitreal ranibizumab (Lucentis) for neovascular age-related macular degeneration. *Am J Ophthalmol*. 2007;143(4):566-583.
- Regillo CD, Brown DM, Abraham P, et al. Randomized, double-masked, sham-controlled trial of ranibizumab for neovascular age-related macular degeneration: PIER Study year 1. *Am J Ophthalmol*. 2008;145(2):239-248.
- Martin DF, Maguire MG, Ying GS, Grunwald JE, Fine SL, Jaffe GJ; CATT Research Group. Ranibizumab and bevacizumab for neovascular age-related macular degeneration. *N Engl J Med*. 2011;364(20):1897-1908.
- Busbee BG, Ho AC, Brown DM, et al; HARBOR Study Group. Twelve-month efficacy and safety of 0.5 mg or 2.0 mg ranibizumab in patients with subfoveal neovascular age-related macular degeneration. *Ophthalmology*. 2013;120(5):1046-1056.
- Chakravarthy U, Harding SP, Rogers CA, et al; IVAN study investigators. Alternative treatments to inhibit VEGF in age-related choroidal neovascularisation: 2-year findings of the IVAN randomised controlled trial. *Lancet*. 2013;382(9900):1258-1267.
- Moutray T, Alarbi M, Mahon G, Stevenson M, Chakravarthy U. Relationships between clinical measures of visual function, fluorescein angiographic and optical coherence tomography features in patients with subfoveal choroidal neovascularisation. *Br J Ophthalmol*. 2008;92(3):361-364.
- Jaffe GJ, Martin DF, Toth CA, et al; Comparison of Age-Related Macular Degeneration Treatments Trials Research Group. Macular morphology and visual acuity in the Comparison of Age-Related Macular Degeneration Treatments Trials. *Ophthalmology*. 2013;120(9):1860-1870.
- Simader C, Ritter M, Bolz M, et al. Morphologic parameters relevant for visual outcome during anti-angiogenic therapy of neovascular age-related macular degeneration. *Ophthalmology*. 2014;121(6):1237-1245.
- Ting TD, Oh M, Cox TA, Meyer CH, Toth CA. Decreased visual acuity associated with cystoid macular edema in neovascular age-related macular degeneration. *Arch Ophthalmol*. 2002;120(6):731-737.
- Schmidt-Erfurth U, Waldstein SM, Deak GG, Kundi M, Simader C. Pigment epithelial detachment followed by retinal cystoid degeneration leads to vision loss in treatment of neovascular age-related macular degeneration. *Ophthalmology*. 2015;122(4):822-832.
- Patel PJ, Chen FK, Rubin GS, Tufail A. Intersession repeatability of visual acuity scores in age-related macular degeneration. *Invest Ophthalmol Vis Sci*. 2008;49(10):4347-4352.
- Pelosini L, Hull CC, Boyce JF, McHugh D, Stanford MR, Marshall J. Optical coherence tomography may be used to predict visual acuity in patients with macular edema. *Invest Ophthalmol Vis Sci*. 2011;52(5):2741-2748.
- Liu M, Wang P-W, Haskova Z. Baseline predictors of early visual acuity improvement in RVO patients treated with ranibizumab in the SHORE study. *Invest Ophthalmol Vis Sci*. 2015;56(7):5802.
- Sophie R, Lu N, Campochiaro PA. Predictors of functional and anatomic outcomes in patients with diabetic macular edema treated with ranibizumab. *Ophthalmology*. 2015;122(7):1395-1401.
- Schlegl T, Waldstein SM, Vogl WD, Schmidt-Erfurth U, Langs G. Predicting semantic descriptions from medical images with convolutional neural networks. *Inf Process Med Imaging*. 2015;24:437-448.
- Willoughby AS, Ying G-S, Toth CA, et al; Comparison of Age-Related Macular Degeneration Treatments Trials Research Group. Subretinal hyperreflective material in the Comparison of Age-Related Macular Degeneration Treatments Trials. *Ophthalmology*. 2015;122(9):1846-1853, e5.
- Hoerster R, Muetter PS, Sitniska V, Kirchhof B, Fauser S. Fibrovascular pigment epithelial detachment is a risk factor for long-term visual decay in neovascular age-related macular degeneration. *Retina*. 2014;34(9):1767-1773.
- Ristau T, Keane PA, Walsh AC, et al. Relationship between visual acuity and spectral domain optical coherence tomography retinal parameters in neovascular age-related macular degeneration. *Ophthalmologica*. 2014;231(1):37-44.
- Kim YM, Kim JH, Koh HJ. Improvement of photoreceptor integrity and associated visual outcome in neovascular age-related macular degeneration. *Am J Ophthalmol*. 2012;154(1):164-173, e1.
- Montuoro A, Wu J, Waldstein S, et al. Motion artefact correction in retinal optical coherence tomography using local symmetry. *Med Image Comput Comput Assist Interv*. 2014;17(pt 2):130-137.
- Wu J, Gerendas BS, Waldstein SM, Langs G, Simader C, Schmidt-Erfurth U. Stable registration of pathological 3D SD-OCT scans using retinal vessels. Paper presented at: Ophthalmic Medical Image Analysis First International Workshop; September 14, 2014; Boston, MA.